ACS APPLIED MATERIALS & INTERFACES

Research Article

www.acsami.org

Nanoporous Polymeric Nanofibers Based on Selectively Etched PS-*b*-PDMS Block Copolymers

Gokcen B. Demirel,[†] Fatih Buyukserin,[‡] Michael A. Morris,[§,⊥] and Gokhan Demirel*[,†,#]

[†]Bio-inspired Materials Research Laboratory (BIMREL), Department of Chemistry, Gazi University, 06500 Ankara, Turkey

[‡]Department of Biomedical Engineering, TOBB University of Economics and Technology, 06560 Ankara, Turkey

[§]Centre for Research in Nanostructures and Nanodevices (CRANN), Trinity College Dublin, Dublin, Ireland

[⊥]Department of Chemistry, University College Cork, Cork, Ireland

[#]Biyomedtek: Center for Bioengineering, 06532 Ankara, Turkey

ABSTRACT: One-dimensional nanoporous polymeric nanofibers have been fabricated within an anodic aluminum oxide (AAO) membrane by a facile approach based on selective etching of poly(dimethylsiloxane) (PDMS) domains in polystyrene-*block*-poly(dimethylsiloxane) (PS-b-PDMS) block copolymers that had been formed within the AAO template. It was observed that prior to etching, the well-ordered PS-*b*-PDMS nanofibers are solid and do not have any porosity. The postetched PS nanofibers, on the other hand, had a highly porous structure having about 20−50 nm pore size. The nanoporous polymeric fibers were also employed as a drug carrier for the native, continuous, and pulsatile drug release using Rhodamine B (RB) as a model drug. These studies showed that enhanced drug release and tunable drug dosage can be achieved by using ultrasound irradiation.

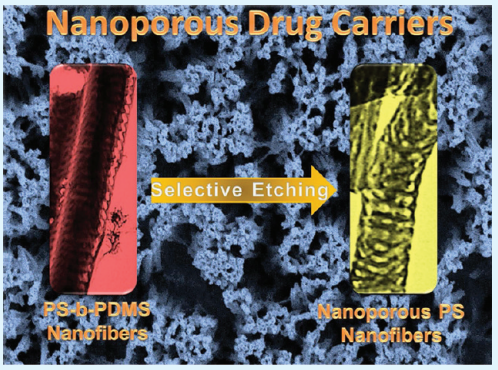

KEYWORDS: *block copolymer self-assembly, anodic alumina membrane, nanoporous materials, ultrasound triggered drug delivery*

INTRODUCTION

The design and development of an effective drug delivery system involves challenges from material science and medicinal perspectives. In a perfect case, a drug delivery system should be able to provide predictable and reproducible release rate.[1−3] However, in some clinical situations like diabetes mellitus, hormone-related diseases, and cancer therapy, an on/off type or a pulsatile drug delivery is required.[4,5] Many external stimuli such as pH, temperature, and different biological agents may be used for this aim, but the control of these impulses presents formidable challenges. Noninvasive ultrasound is probably the most promising external stimuli for on-demand drug delivery where simple manipulation of the ultrasound irradiation time or frequency allows precise control over dosage and drug release.[6]

Polymeric nanoporous materials are a unique class of alternative drug release platform that attract increasing interest because of their large surface area, controllable porosity and ease of chemical functionalization. In addition to applications in effective drug delivery systems, they have also been exploited for several other areas including separation, sensors, catalysis and templates for electronic devices.[7−10] Most of these applications require fine shape control, well-defined pore size, and three-dimensionally continuous pore network. In general, polymeric nanoporous materials can be prepared by mold replication,[11] colloidal lithography,[12] electrospinning,[13] lithography,[14] templating,[15] chemical vapor polymerization,[16,17] and self-assembly.[18] However, these approaches are mostly quite complex, expensive, and slow. Block copolymers offer a wide variety of microphase separated morphologies (e.g., lamellae, hexagonally packed cylinders, bicontinuous double gyroid, cylindrical structure), which are generated by the block immiscibility and connectivity.[10,19] By applying basic techniques such as selective chemical etching,[20] UV irradiation,[21] solvent annealing,[22] or thermal treatment,[23] block copolymers having nanoporous structures can be easily fabricated.

The selective etching of the material of interest in this study, namely, PS-*b*-PDMS block copolymers, is first reported by Ndoiet et al. where the PDMS domains of PS-*b*-PDMS copolymer films were selectively removed by hydrofluoric acid (HF) treatment.[20] However, in their work, they only demonstrated this approach for quite thick films (∼0.5 mm) without investigating their phase separation before and after etching process. To the best of our knowledge, there is no report on the selective etching of microphase separated PS-b-PDMS block copolymeric nanofibers and their use for native or ultrasound-triggered drug delivery.

Combining block copolymers with a template-directed approach can allow the production of monodisperse 1D nanofibers with unique chemical and physical properties at significantly high yields. Herein, we report such an approach to fabricate nanoporous polymeric nanofibers based on microphase-separated PS-*b*-PDMS block copolymers within AAO

Received: September 28, 2011
Accepted: November 22, 2011
Published: November 22, 2011

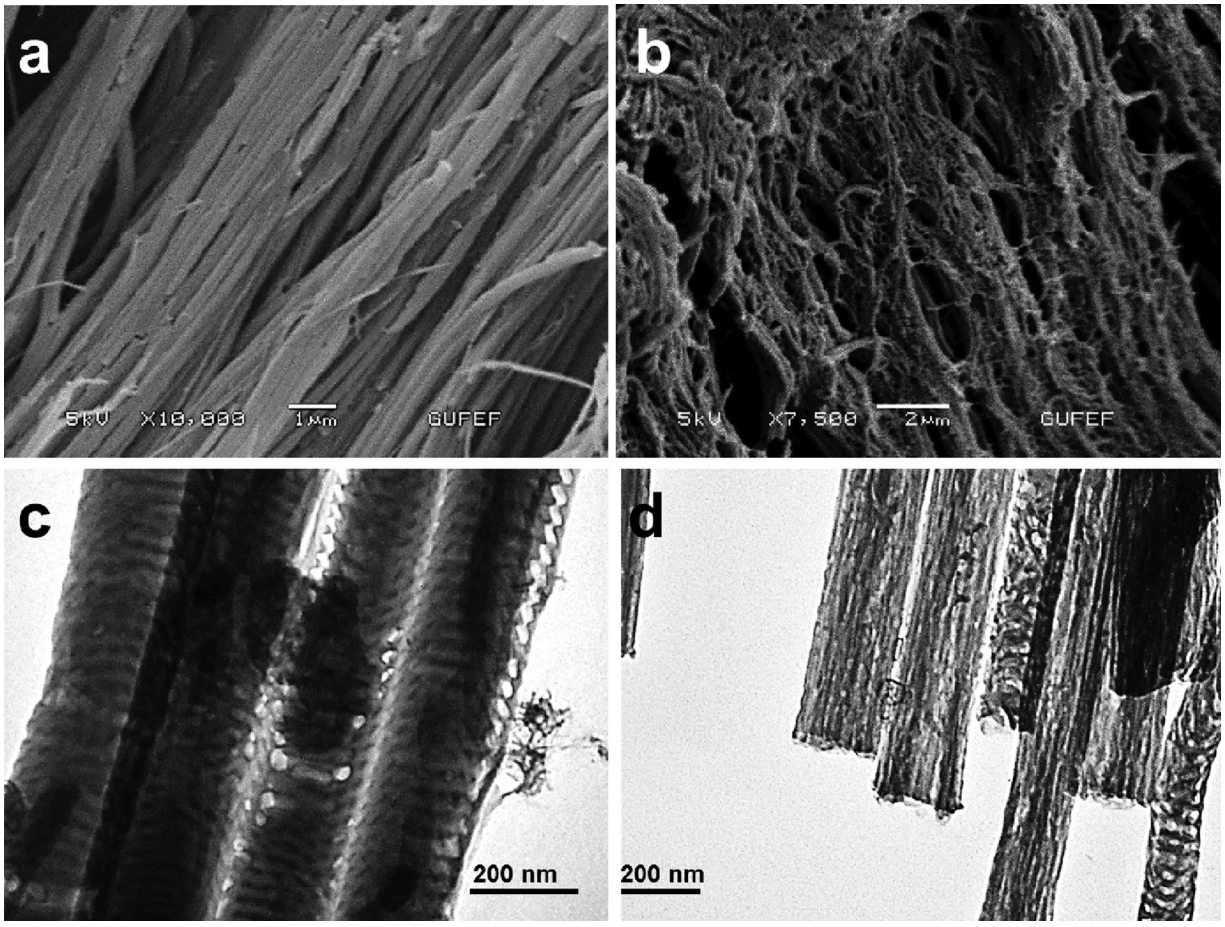

Figure 1. SEM and TEM images of PS-*b*-PDMS nanofibers (a,c) before and (b,d) after selective removal of PDMS domains.

membranes, and subsequent selective etching of PDMS domains from PS-*b*-PDMS nanofibers. These nanoporous polymeric fibers were also employed as a drug carrier for the native, continuous, and pulsatile drug release. Ultrasound was used as an external stimulus.

EXPERIMENTAL SECTION

Fabrication of Nanoporous and Nonporous Polymeric Nanofibers. Polymeric nanofibers were fabricated by template-directed approach using AAO membranes having pore diameters of 200 nm and a thickness of 60 μm (Whatman, Inc.). About 50 mg of PS-b-PDMS (PS block with a number-average molecular weight M_n = 31 00 g/mol - PDMS blocks with M_n = 14 00 g/mol, and the polydispersity index of PS-*b*-PDMS was 1.15 (M_w/M_n)) was first placed on the AAO membrane and heated up to 215 °C in a vacuum oven for 24 h. The excess polymer was removed from the top of the AAO membrane using a scalpel and AAO was removed by immersing into 5.0 M NaOH for 3 h. Individual nanofibers were collected from the mixture by three cycles of centrifugation (12 000 rpm, 180 s), supernatant removal, and redispersion in 5.0 M NaOH. Subsequently, PS-*b*-PDMS nanofibers were immersed into an HF solution (38−40%, v/v) to remove the PDMS domains. After 24 h, they were removed via centrifugation and washed with DI water several times and dispersed in ethanol. The samples were then characterized using scanning electron microscopy (SEM, JSM-6060 JEOL) and transmission electron microscopy (TEM, FEI Tecnai G^2 Spirit).

Loading and Release of Rhodamine B. RB was used as a model drug to evaluate the drug loading and release efficiencies of both nanoporous and nonporous polymeric nanofibers. For a typical loading procedure, both powders of nanoporous or nonporous polymeric nanofibers (~4.0 mg) were placed onto a UV cuvette, and then 3 mL of RB solution (10 mg/mL in DI water) was added into the cuvette. UV-spectra of RB solution were monitored time to time during 24 h at room temperature with a UV−vis spectrometer, and the amount of loaded RB was calculated from the calibration curve of RB using absorbance of RB at 554 nm. The RB loaded samples were then separated through centrifugation at 12000 rpm for 5 min and carefully washed with DI water.

To investigate the natural release of RB from both nanoporous and nonporous polymeric nanofibers, ~4.0 mg of RB loaded sample were placed into a UV cuvette and DI water was added (3 mL). UV spectra of RB were then monitored time to time for 24 h. Ultrasound-triggered drug release studies were also carried out by applying two different methodologies (continuous and pulsatile). For continuous release of RB, drug loaded samples were exposed to ultrasound for 5, 15, and 30 min. Subsequently, they were centrifuged and amount of released RB was determined. Pulsatile drug release was also conducted applying ultrasound irradiation in on/off condition (on for 10 min and off for 10 min). At the end of the each period, released RB was determined as mentioned above. The frequency of the ultrasound and average sonic power for both cases were 42 kHz (± 6.0%) and 70 W.

RESULTS AND DISCUSSION

Figure 1a,b shows the SEM images of PS-b-PDMS nanofibers before and after the selective HF etching procedure. It is evident that prior to the selective etching of the PDMS domains, the PS-b-PDMS nanofibers having about 200 nm diameter are solid and do not have any obvious porosity (Figure 1a). The nanofibers are of uniform width and length indicating good replication of the original AAO structure. It would be expected that these fibers would consist of a hexagonal arrangement of linear PDMS domains within a PS

dx.doi.org/10.1021/am201331b | ACS Appl. Mater. Interfaces 2012, 4, 280−285

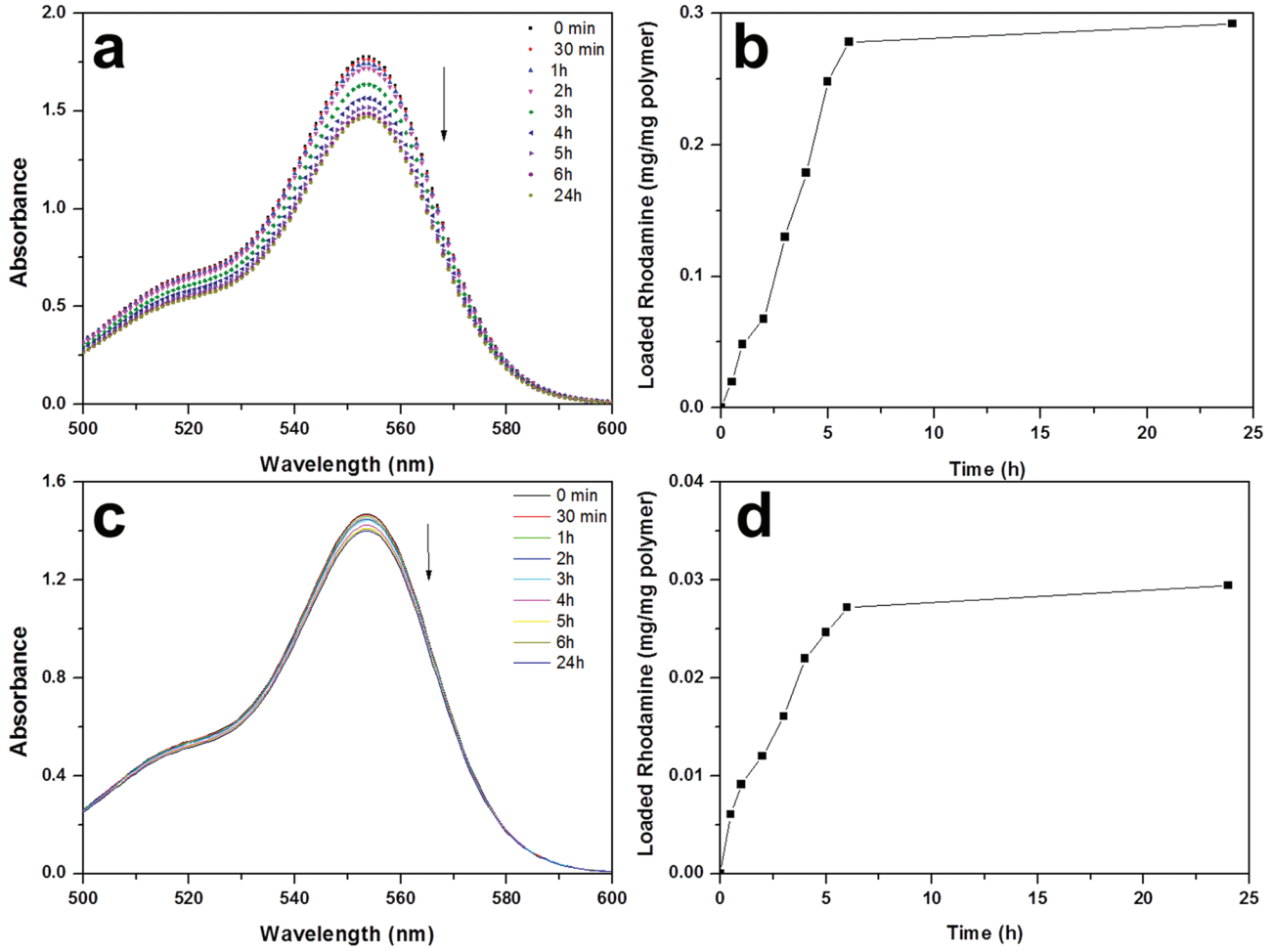

Figure 2. UV absorption spectra of RB solution in (a) selectively etched PS-b-PDMS nanofibers, and (c) nonetched nanofibers. The time-dependent cumulative loading plots (b) for etched nanofibers and (d) for nonetched nanofibers.

matrix[24,25] but the microphase separated structure cannot be resolved by electron microscopy because of the similar image contrast of the two polymers. After selective etching it would be expected that the microphase separated structure would be revealed. It is clear from Figure 1b that HF has changed the nanofibers on both the micro and nanoscale. It is clear that the selective etch has caused some changes in the PS structure and caused some disruption and connections between the aligned nanofibers to occur.[26] This microporosity is probably an advantage in mass transport in these systems. However, TEM studies reveal nanoscale porosity deriving from selective PDMS solution and the nanofibers have a well-defined pore structure of about 20−50 nm of mesh size (Figure 1c,d). It is apparent that these pores are aligned both horizontally and vertically to the nanofiber length (Figure 1d). Moreover, polymeric nanofibers before and after the etching have a thin continuous layer presumably formed by PS part of PS-*b*-PDMS (Figure 1c,d). It is possible to assume that PS components in PS-*b*-PDMS preferentially wet the AAO walls and formed a thin layer during the phase separation. This continuous PS layer probably does not represent a significant diffusion barrier for HF and its degradation products. These results are somewhat contrary to previous reports. It is clear from Figure 1 that the cylindrical PDMS domains have the expected hexagonal arrangement of microphase separation in thin films. Wang et al. reported that the presence of AAO membrane influences the phase separation in block copolymers and may lead to form a lamellar phase in the proximity of the surface even if they have a hexagonal bulk morphology.[26] This apparent contradiction may arise from a number of factors. The phase-separated and alignment of the structure is strongly dependent on the interaction of the surface with the polymer and this is highly dependent on the surface chemistry.[27] In this way, solvent, temperature, polymer concentration, and surface pretreatment can affect the structure observed.

To investigate the release of RB, we first loaded the nanoporous and nonporous polymeric nanofibers with the dye by immersing the fibers into an RB solution at ambient temperature in a dark room, and absorbance of the RB solution was monitored time to time during 24 h. As the RB molecules adsorb onto the polymeric nanofibers, a decrease in the intensity of the RB solution's absorption spectra was observed (Figure 2a). This figure shows the periodically recorded absorption spectra of the RB solutions using nanoporous and nonporous polymeric nanofibers. It is clearly seen that the nanoporous PS-*b*-PDMS nanofibers adsorbed about 10-fold the amount of RB molecules compared to nonporous form (Figure 2a,b). The time-dependent RB loading for both samples was plotted in Figure 2c,d through a RB calibration curve. These data show that in addition to overall enhancement in the loaded RB amount, the nanoporous fibers also display a significant higher adsorption rate when compared with the nonporous

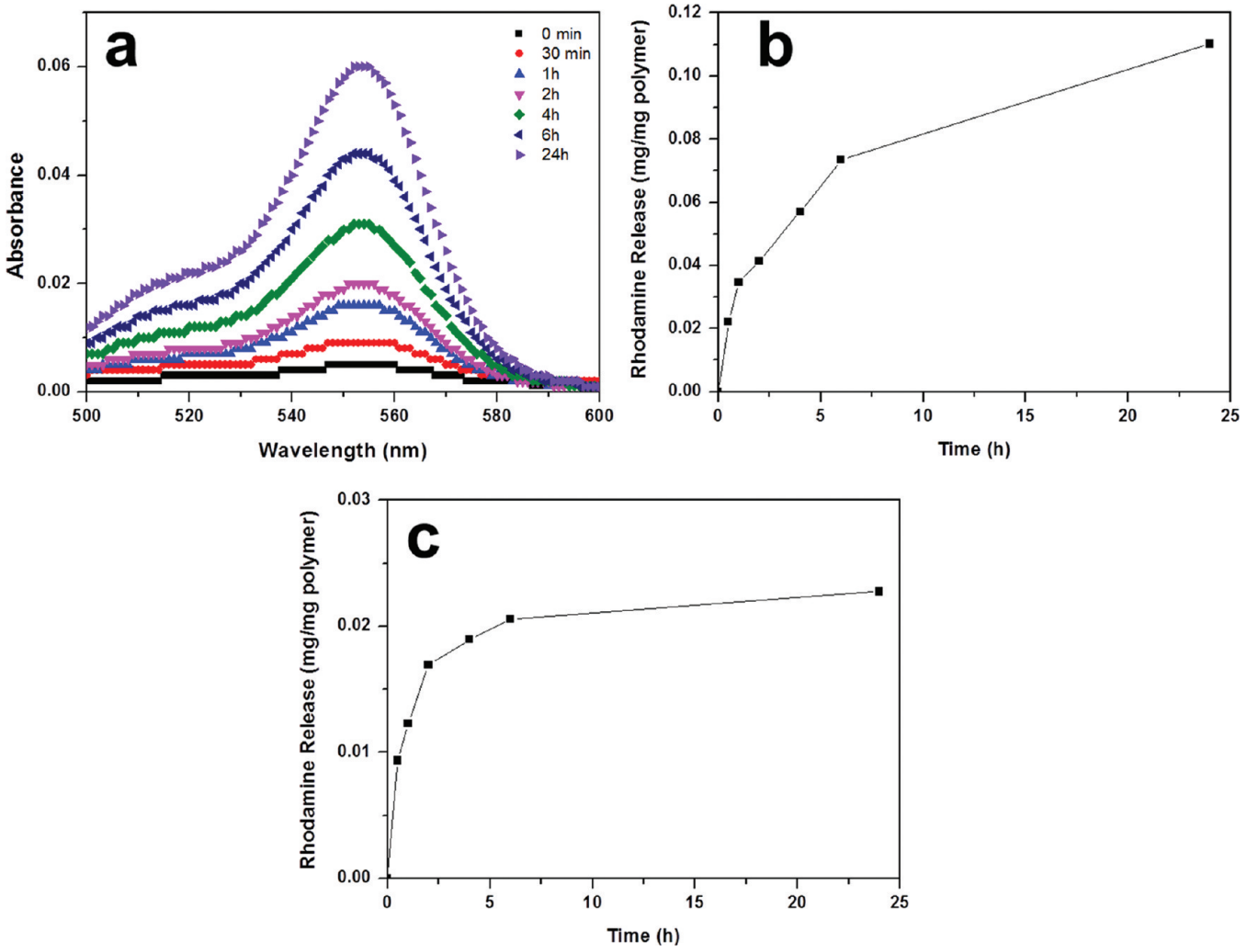

Figure 3. (a) UV spectra of RB from selectively etched PS-*b*-PDMS nanofibers.The cumulative release of RB from (b) nanoporous nanofibers and (c) nonporous nanofibers.

forms did. The adsorption rate for both cases also decreased as the loading process is saturated. The rapid loading might be dominated by diffusion as there is, initially, a concentration gradient and as the length scale for diffusion of RB from solution to the interior of the nanofibers are short.

Two experiments were conducted to investigate the influence of the porous structure on the release of RB: (a) natural release and (b) ultrasound-triggered release. Figure 3a shows the released RB absorbance during the natural release experiments of nanoporous polymeric nanofibers. The slow increase in absorption intensity indicates that there was a relatively slow but sustained release of RB. This is somewhat unexpected considering the rapid adsorption of RB molecules at the early stage of the loading process (Figure 2), which may have been predicted to yield a similarly fast release pattern. The observed tendency may be attributed to highly nanoporous structure of nanofibers where the pore structure causes rapid uptake by capillary flow during adsorption but a mass transport limited resolution of RB during release. Meanwhile, it is also possible to assume that release could be delayed by specific interactions between the RB molecules and PS parts or residual PDMS moieties in nanofibers. To substantiate our conclusion, nonporous polymeric nanofibers were also employed for dye release studies. It is found that RB release from nonporous polymeric fibers increased initially that implies a burst release and then reached a plateau value in about 4 h (Figure 3c). This is consistent with RB being adsorbed at the surface of the fibers and mass transport, therefore, having a lesser effect.

In the first part of ultrasound-triggered release, we examined the influence of continuous ultrasound on the release pattern for RB-loaded nanoporous polymeric fibers (Figure 4a). A proportional increase in the released dye content was observed with increasing irradiation time and a much faster release rate was obtained compared with 'unaccelerated' release experiments. In the case of 5 min irradiation time, RB-loaded nanoporous polymeric nanofibers released about 14% of the dye. Notice that, the same amount of dye could be released after 2 h in the natural release mode (i.e., in the absence of ultrasound). Moreover, it has been observed that the amount of released RB increased to 22 and 36% after 15 and 30 min of continuous ultrasound irradiation, respectively (Figure 4b). Hence, it can be inferred from these results that by simple manipulation of the ultrasound irradiation time, drug dosage can be precisely controlled at enhanced drug release conditions. In the literature, it has been well documented that ultrasound can enhance the drug release.[6,28] This kind of enhancement may generally be attributed to cavitation generation by ultrasound irradiation.[6] With the application of ultrasound,

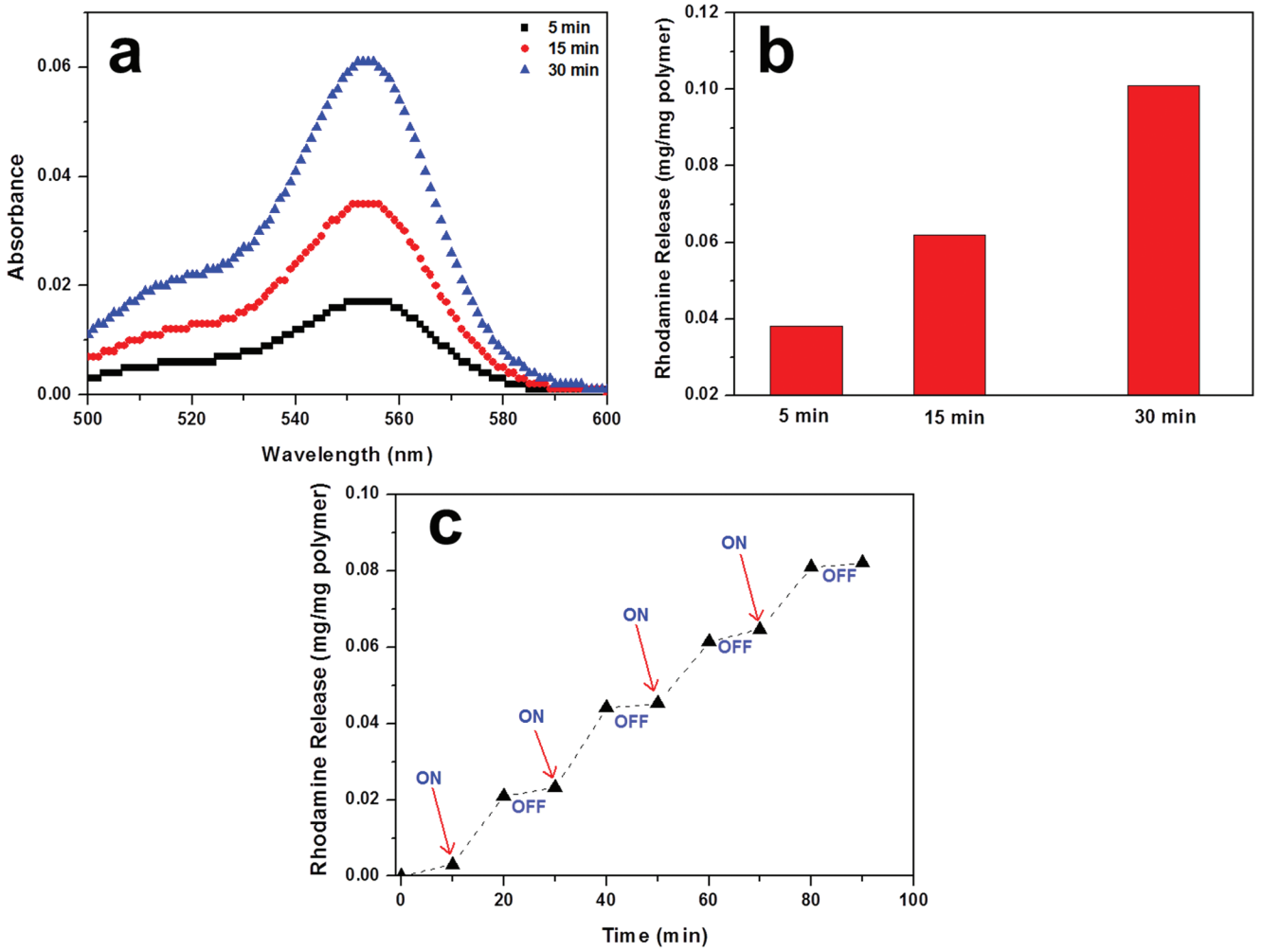

Figure 4. (a) UV spectra of RB from selectively etched PS-*b*-PDMS nanofibers. (b) Cumulative release of RB from nanoporous polymeric nanofibers depending on ultrasound irradiation time. (c) Pulsatile release of RB from nanoporous polymeric fibers (ultrasonic irradiation (10 min) was started at arrows).

microbubble formation and growth occurs as a result of gas/vapor collapse in liquid medium.[29,30] In cavitation, these bubbles mostly concentrate the acoustic energy, which causes the local generation of extreme temperature and pressure.[6] Consequently, ultrasonic cavitation causes convection of the drug, forced diffusion, the improvement of adsorption and/or desorption as well as interior volume and flexibility of the polymer, and hence enhances the drug-release kinetics.

To evaluate the pulsatile RB release from nanoporous polymeric nanofibers, we exposed RB-loaded samples to ultrasound for 10 min. The release of RB started instantly, and continued until the irradiation was stopped (Figure 4c). Pulsatile release of RB was successfully repeated and the amount released in each step was approximately same for each exposure period (~0.02 mg dye/mg polymer). Both continuous and pulsatile drug release data showed that ultrasound irradiation is an effective method for controlled drug delivery. In light of these results, it can be claimed that the nanoporous polymeric fibers fabricated by the selective etching of PS-*b*-PDMS can be potentially used as a smart drug release platform.

CONCLUSIONS

We have demonstrated a simple but versatile method for the fabrication of nanoporous polymeric nanofibers based on selective etching of PDMS domains in PS-*b*-PDMS block copolymers. PS nanofibers having a highly porous structure of about 20−50 nm of mesh size were easily obtained after a selective etching process. The nanoporous polymeric nanofibers exhibited higher and faster RB loading rate compared to nonporous form. Moreover, continuous and pulsatile drug release from RB-loaded nanoporous polymeric fibers showed that by using ultrasound irradiation, enhanced drug release and fine control over drug dosage can be obtained. We believe that such nanoporous polymeric fibers provide greater flexibility not only in the selection of potential drug carriers but also in heterogeneous catalysis, tissue engineering, and biosensors.

AUTHOR INFORMATION

Corresponding Author

*E-mail: nanobiotechnology@gmail.com.

ACKNOWLEDGMENTS

G.D. gratefully acknowledges the Gazi University for the financial supports (Projects 05/2010-83 and 05/2010-17).

REFERENCES

(1) Del Valle, E. M. M.; Galan, M. A.; Carbonell, G. *Ind. Eng. Chem. Res.* **2009**, *48*, 2475−2486.

(2) Brayden, D. J. *Drug Discovery Today* **2003**, *8*, 976−978.
(3) Hughes, G. A. *Nanomedicine* **2005**, *1*, 22−30.
(4) Jeon, G.; Yang, S. Y.; Byun, J.; Kim, J. K. *Nano Lett.* **2011**, *11*, 1284−1288.
(5) Grayson, A. C. R.; Choi, I. S.; Tyler, B. M.; Wang, P. P.; Brem, H.; Cima, M. J.; Langer, R. *Nat. Mater.* **2003**, *2*, 767−772.
(6) Kim, H. J.; Matsuda, H.; Zhou, H.; Honma, I. *Adv. Mater.* **2006**, *18*, 3083−3088.
(7) Rabbani, M. G.; El-kaderi, H. M. *Chem. Mater.* **2011**, *23*, 1650−1653.
(8) Shi, J.; Hsiao, V. K. S.; Huang, T. J. *Nanotechnology* **2007**, *18*, 465501.
(9) Du, X.; Sun, Y.; Bien, T.; Teng, Q.; Yao, X.; Su, C.; Wang, W. *Chem. Commun.* **2010**, *46*, 970−972.
(10) Farrell, R. A.; Petkov, N.; Morris, M. A.; Holmes, J. D. *J. Colloid Interface Sci.* **2010**, *349*, 449−472.
(11) Li, Y. Y.; Cunin, F.; Link, J. R.; Cao, T.; Belts, R. E.; Reiver, S. H. *Science* **2003**, *299*, 2045−2047.
(12) Dalby, M. J.; Berry, C. C.; Riehle, M. O.; Sutherland, D. S.; Agheli, H.; Curtisa, A. S. G. *Exp. Cell. Res.* **2004**, *295*, 387−394.
(13) Lin, J.; Ding, B.; Yu, J.; Hsieh, Y. *ACS Appl. Mater. Interfaces* **2010**, *2*, 521−528.
(14) Hsiao, V. K. S.; Kirkey, W. D.; Chen, F.; Cartwright, A. N.; Prasad, P. N.; Bunning, T. J. *Adv. Mater.* **2005**, *17*, 2211−2214.
(15) Wang, Y.; Caruso, F. *Chem. Mater.* **2006**, *18*, 4089−4100.
(16) Demirel, G.; Malvadkar, N.; Demirel, M. C. *Thin Solid Films* **2010**, *518*, 4252−4255.
(17) Ince, G. O.; Demirel, G.; Gleason, K. K.; Demirel, M. C. *Soft Matter* **2010**, *6*, 1635−1639.
(18) Fery, A.; Scholer, B.; Cassagneau, T.; Caruso, F. *Langmuir* **2001**, *17*, 3779−3783.
(19) Zhou, N.; Bates, F. S.; Lodge, T. P. *Nano Lett.* **2006**, *10*, 2354−2357.
(20) Ndoni, S.; Vigild, M. E.; Berg, R. H. *J. Am. Chem. Soc.* **2003**, *125*, 13366−13367.
(21) Thurn-Albrecht, T.; Schotter, J.; Kastle, G. A.; Emley, N.; Shibauchi, T.; Krusin-Elbaum, L.; Guarini, K.; Black, C. T.; Tuominen, M. T.; Russell, T. P. *Science* **2000**, *290*, 2126−2129.
(22) Wang, Y.; He, C.; Xing, W.; Li, F.; Tong, L.; Chen, Z.; Liao, X.; Steinhart, M. *Adv. Mater.* **2010**, *22*, 2068−2072.
(23) Hedrick, J. L.; Labadie, J.; Russell, T.; Hofer, D.; Wakharker, V. *Polymer* **1993**, *34*, 4717−4721.
(24) Son, J. G.; Hannon, A. F.; Gotrik, K. W.; Katz, A. A.; Ross, C. A. *Adv. Mater.* **2011**, *23*, 634−639.
(25) Yang, J.; Wang, Q.; Yao, W.; Chen, F.; Fu, Q. *Appl. Surf. Sci.* **2011**, *257*, 4928−4934.
(26) Wang, Y.; Gösele, U.; Steinhart, M. *Chem. Mater.* **2008**, *20*, 379−381.
(27) Farrell, R. A.; Fitzgerald, T. G.; Borah, D.; Holmes, J. D.; Morris, M. A. *Int. J. Mol. Sci.* **2009**, *10*, 3671−3712.
(28) Rapoport, N. Y.; Christensen, D. A.; Fain, H. D.; Barrows, L.; Gao, Z. *Ultrasonics* **2004**, *42*, 943−950.
(29) Flint, E. B.; Suslick, K. S. *Science* **1991**, *253*, 1397−1399.
(30) Banks, C. E.; Compton, R. G. *ChemPhysChem* **2003**, *4*, 169−178.